Glacial Troughs Drive Shelf/Slope Exchange

Patrick Hampson[1] and James M. Pringle[1]

[1]University of New Hampshire

November 22, 2022

Abstract

Glacial troughs are flat-bottomed, steep-sided submarine valleys that almost or en-tirely incise the shelf, and significantly alter coastal circulation. When the alongshore flow is in the Kelvin-wave (downwave/downwelling favorable) direction, troughs eject most of the shelf transport offshore to the slope. This offshore ejection diminishes wind-driven alongshore transport downwave of the trough. Conversely, when the alongshore flow isagainst the Kelvin wave direction (upwave/upwelling favorable), the trough moves transport, which had been on the slope, to the shelf, enhancing shelf transport downwave ofthe trough. Troughs enhance offshore ejection by generating relative vorticity, which isdissipated by bottom friction, leading to cross-isobath transport, and by accelerating along-shelf flow, which leads to increased bottom Ekman transport. A barotropic, linear, steady-state model is used to quantify the increased exchange between shelf and slope, as a function of the trough geometry.

Glacial Troughs Drive Shelf/Slope Exchange

Patrick M. Hampson[1], **James M. Pringle**[1]

[1]University of New Hampshire, Ocean Process Analysis Laboratory in the Institute for the Study of Earth, Ocean, and Space and the Department of Earth Science, Durham, NH, USA

Key Points:

- Glacial troughs drive offshore exchange from shelf to slope for downwave/downwelling flows, and onshore exchange for upwelling/upwave flows.
- Trough bathymetry converges shelf isobaths, which causes flows to accelerate and generate relative vorticity.
- Bottom friction dissipates this generated vorticity and drives cross-shelfbreak transport.

Abstract

Glacial troughs are flat-bottomed, steep-sided submarine valleys that almost or entirely incise the shelf, and significantly alter coastal circulation. When the alongshore flow is in the Kelvin-wave (downwave/downwelling favorable) direction, troughs eject most of the shelf transport offshore to the slope. This offshore ejection diminishes wind-driven alongshore transport downwave of the trough. Conversely, when the alongshore flow is against the Kelvin wave direction (upwave/upwelling favorable), the trough moves transport, which had been on the slope, to the shelf, enhancing shelf transport downwave of the trough. Troughs enhance offshore ejection by generating relative vorticity, which is dissipated by bottom friction, leading to cross-isobath transport, and by accelerating alongshelf flow, which leads to increased bottom Ekman transport. A barotropic, linear, steady-state model is used to quantify the increased exchange between shelf and slope, as a function of the trough geometry.

Plain Language Summary

A specific type of submarine valley, the glacial trough, is shown to alter how ocean currents behave within the coastal environment. Computational modeling is used to explore how troughs (of different sizes and shapes) impact coastal circulation for a particular set of physical conditions. Results from this model demonstrate that troughs change coastal circulation by enhancing the movement of shelf waters to the continental slope, as well as slope waters to the shelf (depending on flow conditions). The relative importance of the mechanisms responsible for these dynamics are quantified, and an analysis of the significance of this phenomenon is given. The main implications of these results relate to nutrient cycling and glacial melting.

1 Introduction

Glacial troughs are relatively deep, u-shaped submarine valleys that cross most of the shelf. Troughs, which were usually formed by glaciation, are concentrated at high latitudes: the shelves of the Arctic, Southern Ocean, Greenland, Norway, and others (Harris & Whiteway, 2011). How troughs modify coastal circulation is understudied in the existing literature. However, research exists on how narrowing/widening shelves and river-carved canyons on the continental slope modify coastal circulation (Allen & Hickey, 2010;

Chapman & Gawarkiewicz, 2012; Pringle, 2002; Williams et al., 2001). This existing literature demonstrates that bathymetric control of coastal circulation is important. Extending this type of research to the trough will improve theories of coastal circulation, such as how shelfbreak jets and concentrated slope flows are formed (Chapman, 1986; Fratantoni & Pickart, 2007; Greatbatch et al., 1995; Greenberg & Petrie, 1988; Han et al., 2008).

The Laurentian Channel (a significant trough) has a large impact on the flows over the Scotian Shelf (Sandstrom, 1980). Biological and sediment distribution patterns are altered by the troughs of the Norwegian Shelf (Buhl-Mortensen et al., 2012). These observations demonstrate the importance of understanding trough-driven dynamics.

Understanding how fjords impact coastal circulation will be improved with these results. This is because fjords are submarine valleys that incise into coastlines. The head of the trough starts near or at the coast instead of some distance offshore. Quantifying the circulation of these regions aids in predicting glacial mass-balances. This is because fjords often have sea-ice interfaces, whose instabilities depend on which water masses (warm or cold) penetrate to the head of the trough, near the terminus of the glacier, such as deeper, warmer slope waters (Straneo et al., 2011).

In the barotropic limit, a trough separates the shelf into two regions: the shelf upwave of the trough, and the shelf downwave. Downwave is the propagation direction of long coastal trapped waves, which travel with shallows on their right in the northern hemisphere (Huthnance, 1975); upwave is the reverse direction. The effect of winds on shelf circulation at any alongshore point is due to winds upwave of such flows. At an alongshore point, the structure of a shelf flow is the consequence of all upwave forcing (Csanady, 1978; Pringle, 2002). Therefore, the upwave shelf circulation is unaltered by the trough, whereas the downwave shelf circulation is impacted by the trough. This study determines how a trough modifies an unperturbed wind-driven flow on the upwave shelf into an adjusted flow downwave of the trough.

A wind-generated shelf flow, for an alongshore uniform shelf and wind forcing, is used as the unperturbed, upwave condition. By studying how troughs modify this wind-generated flow into some downwave-adjusted state, we can better understand the interaction between bathymetric and surface forcing on the shelf. In addition to this forcing upwave of the trough, wind forcing downwave of the trough is also explored. Including these winds downwave of the trough allows for a better understanding of how troughs modify wind-forced shelf circulation downwave of the trough.

2 Methods

2.1 The Conceptual Model

Circulation is modeled on a f-plane shelf (constant Coriolis frequency), where the y-axis points alongshore north and positive x-axis points offshore east. This western boundary shelf's bathymetry is defined to include a trough, as seen in Figure 1.

Waters on this shelf are assumed to be barotropic, i.e., the Rossby radius of deformation, $\frac{\sqrt{g'H}}{f}$ (where g' is the reduced gravity gravitational acceleration defined with the top to bottom stratification, H is depth, and f is the Coriolis frequency), is small compared to the cross-shore length scale of bathymetry variation (Pringle, 2002). Therefore, these results are applicable to either barotropic shelf waters or to barotropic modes of a baroclinic shelf.

Circulation on this shelf is studied in the steady-state limit, which assumes that the flow has fully adjusted to its forcing, and that the forcing itself is steady. Because wind-driven flows are used, the timescale of adjustment is the frictional spin-down time: $\frac{H}{r}$ (Williams & Carmack, 2008), where r is the linear drag coefficient. For the model parameters chosen, this timescale is of O(2-3 days) at the shelfbreak; beyond this timescale, flows are at a fully-adjusted steady-state.

Flows are assumed to be linear, or at small Rossby number, i.e., $\frac{u}{fL} << 1$, where u is the velocity of flows and L is its length scale of variation. Because linear flows follow isobaths at lowest order, a flow acceleration occurs where the isobaths narrow – for example, between the coast and the trough head. This convergence accelerates the flow towards a nonlinear regime. This model properly describes where and how these linear flows approach a nonlinear state. However, the detailed structure of any nonlinear flows is not properly described when $\frac{u}{fL}$ is of O(1), or greater.

A linear bottom friction is used, which averages over frictional variations at higher frequencies than the assumed steady-state timescale: tides, surface gravity waves, etc. (Csanady, 1978; Greenberg & Petrie, 1988). This approximation assumes bottom drag to be directly proportional to the depth-integrated velocity of the geostrophic interior.

This is reasonable, given that these waters are both barotropic and at steady-state. Furthermore, the use of a linear bottom friction has replicated observations at lowest order (Brink & Allen, 1978; Lentz et al., 1999; Wright & Thompson, 1983). The bottom stress is

$$\vec{\tau_{bot}} = \rho_0 r \frac{\vec{U}}{H}, \tag{1}$$

where τ_{bot} is the bottom frictional stress, ρ_0 is the standard density of water, r is the linear drag coefficient, $\vec{U}$ is the depth-integrated velocity, and H is the depth of water columns.

The aggregate of these assumptions comprises a model that has been explored by various studies (Chapman, 1985, 1986; Csanady, 1978; Gordon, 1982; Pringle, 2002; Sandstrom, 1980; Williams & Carmack, 2008). They lead to momentum and continuity equations of the following form:

$$\begin{aligned} -fV &= -gH\eta_x + \frac{\tau^x_{top}}{\rho_0} - \frac{\tau^x_{bot}}{\rho_0} && (2)\\ fU &= -gH\eta_y + \frac{\tau^y_{top}}{\rho_0} - \frac{\tau^y_{bot}}{\rho_0} && (3)\\ U_x + V_y &= 0, && (4) \end{aligned}$$

where U and V are the depth-integrated cross and alongshore transports, respectively, η is the surface elevation function, and $\tau^x_{top,bot}$ and $\tau^y_{top,bot}$ are the offshore and alongshore components of the surface and bottom stresses, respectively.

The mass transport streamfunction, $U = \Psi_y$ and $V = -\Psi_x$, satisfy the continuity equation (4). After dividing by the depth, H, cross-differentiation of the remaining two-dimensional momentum equations leads to the vorticity equation (5):

$$0 = J(\Psi, \frac{f}{H}) + \nabla \cdot (\frac{r}{H^2}\nabla\Psi) - \nabla \times (\frac{\tau^{top}}{\rho_0 H}), \tag{5}$$

where J(a,b) is the Jacobian of (a,b). The solution to these equations is governed by their boundary conditions, which are the inflows discussed in the next section.

The vorticity equation is composed of three terms (in order of appearance in equation 5): 1) the advection of potential vorticity, $\frac{f}{H}$, by Ψ, 2) the dissipation of relative vorticity, $\nabla^2\Psi$, by bottom friction, r, and 3) the generation of potential vorticity by the curl of the wind stress, τ^{top}. A direct solver was created to find solutions to this vorticity equation for a given input geometry (constructed on a grid with a 500-meter-offshore by 1-kilometer-alongshore grid spacing) and forcing conditions. The grid spacing was determined by conducting sensitivity tests, where the model was constructed with coarse grid spacing and shrunk until results were no longer dependent on grid spacing changes. A matrix of discrete vorticity equations was constructed for the domain, using central derivatives for the gradients. Boundary conditions were implemented as vorticity equations at the matrix boundaries.

Once these matrix constructions steps were done, a streamfunction was solved for with built-in linear algebra tools of Python. The streamfunction, Ψ, is found in its vector form and then transformed into domain space (x by y):

$$E\Psi = F, \tag{6}$$

where E is the N-by-N equation matrix (where N is equal to the total amount of grid cells of the domain), Ψ is a N by 1 streamfunction vector, and F is the forcing (which may include downwave winds).

The model domain is a northern-hemisphere, western-boundary bathymetry. The underlying bathymetry (excluding the trough) is a hyperbolic tangent sloping to a shelf-break depth of 100 m at approximately 125 km offshore:

$$H_{troughless} = (\frac{H_{sb} - H_{coast}}{L_{sb}}) * (x - L_{sb}) + H_{half} * tanh((x - L_{sb})/L_{slope})^2) + \text{offset}, \tag{7}$$

where H_{sb} is the depth at the shelfbreak, H_{coast} is the nonzero depth at the coast, L_{sb} is the shelf width, x is the offshore dimension, H_{half} is half the depth to the bottom of the slope, L_{slope} is the offshore width of the slope, and "offset" increases the depth by a constant.

This bathymetry, $H_{troughless}$, is constant in the alongshore direction: the trough is superimposed on it. The trough bathymetry is a flat-bottomed hyperbolic tangent function in the cross-shelf direction. The offshore form of the trough bathymetry ($H_{trough,o}$) is:

$$H_{trough,o} = H_{trough} * tanh((x - L_{head})/(L_{slope}/a)^2), \tag{8}$$

where H_{trough} is the trough depth, L_{head} is the offshore distance between the coast and the shoreward head of the trough, and a is a parameter used to further adjust the slope. Standard/baseline values for model bathymetry, as well as values used in variation runs are found in (Table 1) and are plotted in (Figure 1).

Equation (8) gives the cross-shelf form of the trough imposed on the underlying shelf bathymetry. The alongshelf shape of the trough ($H_{trough,a}$) was constructed with:

$$\begin{aligned} H_{trough,a} = (1 - ((1 - 0.5 * (1 - tanh((((y - y_0) - W_{trough}/2)/W_{wall}))) \\ +(1 - 0.5 * (1 - tanh((-(y - y_0) - W_{trough}/2)/W_{wall})))), \end{aligned} \tag{9}$$

where y_0 is the alongshore center of the trough, W_{trough} is the alongshore width of the trough bottom, and W_{wall} is the alongshore width of the trough sidewalls. The functions for the cross-shelf and alongshelf extent of the trough are then combined with the background bathymetry to give the final bathymetry:

$$H = \text{the larger of } (H_{troughless}, H_{trough}). \tag{10}$$

2.2 Boundary Conditions

The flow on a barotropic shelf is forced by winds upwave of a given location on the shelf (Battisti & Hickey, 1984; Csanady, 1978). In order to isolate a trough's alteration of shelf circulation, an initial set of model runs are conducted, where forcing is limited to the shelf upwave of the trough. By neglecting forcing downwave of the trough, the circulation on the shelf downwave of the trough is purely a trough-adjusted state; the response isn't altered by additional forcing.

The upwave boundary's streamfunction is set to the flow forced by an alongshore uniform wind forcing over an infinite alongshore uniform shelf upwave of the model domain. This shelf velocity leads to a balance between bottom friction and alongshore windstress to give:

$$v_{2D} = \frac{\tau^y}{\rho_0 r}, \tag{11}$$

where v_{2D} is the alongshore velocity, τ^y is the alongshore component of the wind stress, ρ_0 is the standard density of water, and r is the linear drag coefficient.

Without wind forcing over the shelf between this upwave boundary and the trough, streamlines of this wind-generated flow would migrate across isobaths in the offshore direction (Csanady, 1978). Therefore, wind forcing over the shelf is included in this region so that these wind-generated flows maintain their structure. These winds were defined to be from the upwave domain border to the upwave edge of the trough, for standard cases. An upwelling-favorable experiment was run with winds over the same area, but directed upwave. Additionally, a two-trough run was conducted with winds over the entire shelf from the upwave to downwave domain boundaries. These experiments are described later in this study. For all wind forcing, the offshore extent ended at the shelf-slope boundary (approximately 125km offshore). This offshore extent was used to avoid unphysically strong flows on the slope, given this study's interest in isolated shelf flow dynamics. The combination of this upwave wind-generated flow boundary condition, and wind forcing between this upwave boundary and the trough, assures that the trough is forced with an unaltered wind-generated shelf flow.

The downwave boundary condition is set to match the upwave condition in all cases. This assures that the transport that enters through the upwave boundary can exit the domain. The impact of the downwave boundary on the internal dynamics is negligible, as its effect is confined to a Stommel distance, i.e., Stommel's scale with topographic beta (Pringle, 2002; Stommel, 1948). This can be derived from scaling (5), giving:

$$L_y = L_{fric} \propto \frac{r}{f H_x}. \tag{12}$$

All plotting of streamline results excludes the 50 km closest to the downwave boundary to ignore the adjustment within this Stommel distance. There is no flow through the coast. This is done by holding the coastal streamfunction to a constant value. The offshore boundary is also set to the no-flow condition by holding its value to a value consistent with the transport through the upwave boundary. The rationale of this choice is twofold: 1) open offshore boundaries are unnecessary for this study because the focus is on isolated shelf dynamics, and 2) even if basin-forced flows came through this boundary, they would steer downwave at the slope and follow isobaths out through the downwave boundary, without penetrating onto the shelf. Isolation of the shelf from basin circulation is due to the steep continental slope, whose vorticity gradient largely insulates the shelf from offshore forcing (Chapman, 1985).

These four boundary conditions are used for all model runs.

2.3 Wind Forcing Downwave of the Trough

The standard model run configuration, which uses wind forcing only upwave of the trough, isolates the trough's impact on upwave wind-generated shelf circulation. An additional set of model runs are used, which includes wind forcing over the entire shelf, i.e., upwave, local, and downwave to the trough.

Results from these runs allow for an insight as to how far downwave from of a trough that its impact remains significant. Winds over this downwave shelf will attempt to regenerate shelf circulation. By observing how far alongshore it takes for a thorough regeneration, the region of the trough influence can be estimated. The combination of the first set of runs, which have wind forcing only upwave of the trough, and these model runs, which have winds over the entire shelf, gives a complete picture of the trough impact.

3 Results

Long coastal trapped waves are the primary mode of transmitting forcing information to downwave waters, being the initiator of flow adjustment. Therefore, a straightforward approach to analyzing how flows adjust in the alongshore direction is by progressing in the long CTW direction from the upwave boundary (with the coast on the right in the northern hemisphere) (Battisti & Hickey, 1984). The examination of model results in this study is primarily conducted through a downwave orientation, i.e., north to south on this western-boundary, northern-hemisphere shelf.

3.1 Trough Ejection Mechanisms

First the effect of a trough on flows forced by downwave, downwelling-favorable winds will be described. Bottom friction acts to move shelf flows across isobaths. This is illustrated with two model runs: one shelf without a trough, and one with a trough (Figure 2). Upwave/north of 300 km in the model, flows that enter through the upwave boundary are maintained with the downwave-oriented wind forcing over the shelf. No winds exist downwave/south of 300 km.

The left panel of Figure 2 shows how streamlines on a trough-less shelf evolve in the alongshore direction, following the ATW dynamic. Downwave of where the winds stop (shown as a red line), streamlines begin to drift offshore. This migration of streamlines towards the slope is greatly increased in the case of a trough, as seen in the right panel. Enhanced offshore migration of shelf flows to the slope by the trough will be referred to as “ejection.”

An ejection metric is defined as the percentage of shelf transport lost offshore beyond the shelfbreak. It is the fraction of the transport that passes through the upwave (red) transect that has moved offshore (beyond the shelfbreak) by the point of the downwave (black) transect:

$$\Delta E = \frac{\Psi_{shelfbreak,downwave}}{\Psi_{shelfbreak,upwave}} * 100 - E. \tag{13}$$

The term ΔE quantifies the additional percentage of shelf transport lost offshore to the slope due to the trough. The transects intersect the shelf from the coast to 125 km offshore at the shelfbreak, and are placed at 100 km and 300 km north of the southern boundary, for the downwave and upwave transects, respectively. These transects were used for calculating this ejection for all single-trough model runs (appropriate transects were chosen for the two-trough runs). E quantifies shelf transport loss but for a shelf without a trough. By subtracting off this value, we calculate the additional ejection caused by the trough. E is approximately 22% for the baseline parameters (left panel of Figure 2).

When the baseline trough is included, an additional 53% of shelf transport is ejected offshore to the slope (right panel of Figure 2). Both this ejection result and the visual evolution of streamlines throughout this trough-shelf system indicates that troughs increase the cross-isobath migration of flows to the slope, all the while sharpening an often-observed shelfbreak jet (Chapman, 1986; Gawarkiewicz & Chapman, 1991).

Enhanced offshore ejection of shelf circulation to the slope is caused by the trough modification of flows from upwave. Upon encountering the trough from the upwave direction, flows steer onshore around the trough, are squeezed into the narrowed shelf, and then are ejected offshore to the slope. Flows are attempting to follow isobaths throughout this progression because linear flows follow isobaths at lowest order (Csanady, 1978). If the alongshore variation in the bathymetry causes the flow to develop relative vorticity, bottom friction will dissipate this vorticity. If, in the northern hemisphere, the relative vorticity is positive, friction will reduce the linear potential vorticity f/H by moving flows across isobaths to deeper water; the converse is true for negative relative vorticity. If the isobaths converge, the isobath-following-flows will accelerate. This will drive an additional cross-shelf transport in the bottom Ekman layer.

To understand the mechanisms that cause the trough to enhance cross-isobath transport, it is useful to write (5) in an along- and cross-isobath coordinate system, following Pringle, 2002. In this coordinate system, n is towards deeper water (and is x where there is no trough), and p is along the isobath (and is y where there is no trough). The cross-shelf transport $\partial\Psi/\partial p$, in the limit that the along-isobath lengthscale of variation in flow is much longer than the cross-isobath lengthscale, can then be written as:

$$\frac{\partial \Psi}{\partial p} = \left[\frac{\partial}{\partial n}\left(\frac{f}{H}\right)\right]^{-1} \times \left[\frac{\partial}{\partial n}\left(\frac{r}{H^2}\frac{\partial \Psi}{\partial n}\right) + \frac{1}{R}\left(\frac{r}{H^2}\frac{\partial \Psi}{\partial n}\right) - \nabla \times \left(\frac{\tau^{\mathbf{top}}}{\rho_0 H}\right)\right], \qquad (14)$$

where R is the radius of curvature of the isobath. The lengthscale assumption is the long-wave assumption of Csanady, 1978, and while it may not be strictly met at the trough, this equation can still be used to gain insight into the dynamics.

The first of three terms in brackets on the right-hand side represents the frictional dissipation of relative vorticity caused by the cross-isobath gradient in the along-isobath flow, as well as the cross-isobath transport in the bottom Ekman layer. In this case where the along-isobath flows upwave of the trough have a constant velocity, the former is governed by the second-derivative of bathymetry in the cross-shelf direction, while the latter is enhanced when narrowing isobaths accelerate the flow. The second term represents the frictional dissipation of the relative vorticity caused by flow moving along curving isobaths with a radius of curvature R. These terms are discussed at length in Pringle, 2002.

To estimate the magnitude of these terms around the trough, one can assume that the flow is along isobaths. Clearly this cannot be true everywhere, as the trough moves streamlines across the shelf, but it can be used to start to understand the dynamics. Upwave of the trough, the alongshore flow v is given by (11) and the bottom slope is α, which will be approximately $L_{shelf}/H_{shelfbreak}$. This leads to:

$$v = \frac{1}{H}\frac{\partial \Psi}{\partial n} = v_{2D}\frac{1}{\alpha}\frac{\partial H}{\partial n}, \qquad (15)$$

which says that the along-isobath velocity will increase in proportion to the narrowing of the isobaths. This can be substituted into (14), along with (11), to find the cross-isobath transport due to isobath narrowing:

$$\left.\frac{\partial \Psi}{\partial p}\right|_{\text{narrowing}} = -\left(\frac{\tau^y_{\text{upwave}}}{\rho_0 f}\right) H^2 \left(\frac{\partial H}{\partial n}\right)^{-1} \left[\frac{\partial}{\partial n}\left(\frac{1}{\alpha H}\frac{\partial H}{\partial n}\right)\right], \qquad (16)$$

and due to the curvature of the isobaths:

$$\left.\frac{\partial \Psi}{\partial p}\right|_{\text{curving}} = -\left(\frac{\tau^y_{\text{upwave}}}{\rho_0 f}\right) H^2 \left(\frac{\partial H}{\partial n}\right)^{-1} \left[\frac{1}{R}\left(\frac{1}{\alpha H}\frac{\partial H}{\partial n}\right)\right], \qquad (17)$$

where both transports scale with $\frac{\tau^{y}_{\text{upwave}}}{\rho_0 f}$, the surface Ekman transport driven by the wind upwave of the trough.

From (16) and (17), the dependence of the fraction of the along-shelf transport moved off the shelf (for downwave flows), or onto the shelf (for upwave flows), on bottom friction, and the Coriolis parameter, can be estimated. Upwave of the trough, the transport on the shelf will scale as its area multiplied by the alongshore velocity on the shelf upwave of the trough from (11), or approximately $0.5{*}L_{shelf}{*}H_{shelfbreak}v_{2D}$. The ratio of either (16) or (17) to this transport scales as rf^{-1}, and so the fraction of the shelf water transported across isobaths onto or off the shelf by the trough is expected to depend on rf^{-1}. This is verified in Figure 3, where the model is run for different values of r and f, and the fraction of the transport ejected offshore is shown to depend on this ratio.

Equations (16) and (17) can also be used to explore the relative importance of curvature and isobath narrowing to understand which mechanism is most important. In Figure 4, the relative strengths of the two sources on cross-isobath transport are shown for the base case, both over the entire shelf (panels A and B), and along the isobath bounding the shelf (panel C). It is clear from these plots that the contribution to cross-isobath transport due to isobath converging near the trough is much greater than that due to isobath curvature. This is true for all parameter runs given in this paper. Even where the curvature term is locally greater - for example, mid-shelf - it tends to cancel itself out when integrated along an isobath. This cancellation occurs because as one moves downwave from the northern boundary, negative curvature along an isobath as it curves into a trough is canceled by positive curvature along the isobath at the inshore end of the trough. A similar cancellation occurs as the isobath leaves the trough. For the analysis below, attention will be concentrated on the effects of narrowing isobaths on cross-isobath transport, because it is the dominant term for this geometry.

The next section explores the dependence of shelf/slope transport exchange, as a function of the trough geometry.

3.2 Relative Importance of the Trough Parameters to Offshore Ejection in the Downwave/Downwelling-Favorable Case

To understand how shelf/slope exchange depends on the geometry of the trough, a series of model runs is made varying a single parameter at a time, while holding all others to their baseline values (Table 1). These are used to quantify offshore ejection of shelf flow as a function of non-dimensional parameter groups (Price, 2003). As described above, these ejection metric results for trough cases are calculated as "additional" offshore ejection (13), beyond the background shelf transport loss caused by the ATW-dynamic of a trough-less shelf (Csanady, 1978). See Figure 1, which introduced the bathymetric schematic of this model, for the relevant parameters.

Two parameters control the spatial extent of regions with narrowed isobaths: $\frac{L_{head}}{L_{shelf}}$, and $\frac{W_{trough}}{L_{shelf}}$, where L_{head} is the offshore distance of the narrowed shelf, L_{shelf} is the offshore distance of the entire shelf, and W_{trough} is the alongshore distance of the trough's base (Figure 1). The first parameter group ($\frac{L_{head}}{L_{shelf}}$, measuring distance between the trough and shelf) indicates the strength of flow shear, i.e., the narrowing mechanism at the coastal end of the trough. As the narrowed shelf becomes wider, until the trough disappears to the slope, this shear effect will become less and less significant. The second parameter group ($\frac{W_{trough}}{L_{shelf}}$, measuring the relative alongshore size of the trough) accounts for the accumulation of the shear effect. A larger alongshore width of the trough gives more distance for the effect of narrowed isobaths to accumulate (Figure 5).

The left panel of Figure 5 plots the first parameter group of the narrowing source ($\frac{L_{head}}{L_{shelf}}$), i.e., shear strength. As the parameter reaches one, the trough disappears to the slope. As this narrowed shelf approaches the total shelf width, the additional ejection caused by the trough reduces to zero, confirming that the trough-less shelf converges to the ATW value. For small values of $\frac{L_{head}}{L_{shelf}}$, the trough bisects the entire shelf. A full shelf intersection leads to an additional 60% of the shelf flow being ejected offshore to the slope in the base case.

The right panel of Figure 5 plots the second parameter group ($\frac{W_{trough}}{L_{shelf}}$). As the parameter approaches unity, the alongshore trough width becomes the same distance as the entire shelf width (120 km), and 70% of the shelf flow is ejected to the slope. As W_{trough} increases in length, there is more alongshore distance for cross-isobath transport along the coastal edge of the trough, and thus more transport is moved from the shelf to the deep walls of the trough, and then the slope. As the parameter goes to zero, the trough disappears, and ejection converges to the background ATW value. Both of these narrowing source parameter groups change offshore ejection by 60-70% for an O(1) change in parameter.

The effects of the change in trough depth are also shown (Figure 6). These results show that as the trough depth increases, the offshore ejection increases; this has the same functional form and O(1) impact as that of the narrowing mechanism. As the trough becomes deeper, the steepness of its sides increases, causing greater isobath convergence and increased cross-isobath transport.

Other trough parameters have less of an impact but follow a similar pattern: as trough geometry changes to increase bathymetric steepness and the convergence of isobaths, more of the shelf transport is moved to the slope in the downwave flow case.

3.3 Alongshore Response Scale of Wind Forcing versus Trough Ejection Impact

The alongshore, downwave shelf winds counteract the offshore ejection caused by troughs. Downwave of the trough, the alongshore winds begin to the reestablish the alongshore wind driven flow, with the flow eventually ceasing to be affected by the trough some distance downwave of the trough. This is demonstrated with model results of a shelf with alongshore-uniform shelf winds. These model runs are made with a 2000 km shelf so that the difference in the alongshore scales of both wind forcing and trough-induced offshore ejection can be compared. Two runs are compared for this this longer shelf: one with a single trough near the upwave boundary, and one with two troughs separated across the alongshore expanse of the shelf.

Figure 7 shows the results of these cases, with a one-trough run shown on the left and a two-trough run shown on the right. The ejection results shown in the headers are normalized with the resulting ATW offshore ejection of this 2000 km shelf without a trough, giving ejection beyond that standardized value. The cross-shore transects used to calculate the change in shelf transport were placed upwave of the first trough and near the downwave boundary (shown with red and black transects, respectively). The significant alongshore distance of these runs allows for an understanding of how the trough impact evolves far downwave from the trough itself. The one-trough case shows a 9% enhanced offshore ejection of shelf transport to the slope at an alongshore distance of approximately 1500 km downwave of the trough. This demonstrates that the trough ejection is largely “forgotten” by this point downwave. The two-trough case shows a 44% enhanced offshore ejection of shelf transport to the slope. These results show that the alongshore scale it takes for winds to regenerate shelf transport is much larger than the scale it takes for a trough to eject such transport offshore.

These model results demonstrate that trough ejection is acting on an alongshore scale of O(10's km). Wind forcing, however, acts on an alongshore scale - corresponding to how far in the alongshore it takes winds to fully re-establish shelf circulation - that scales as: $L_{fric} = -\frac{Hf}{2r}L^x$, where L^x is the offshore length scale (Chapman, 1986; Pringle, 2002). At the shelfbreak, which is the relevant cross-shelf length scale for considering the entire shelf's circulation state, this frictional scale is O(1500 km). Given that the trough ejection scale is approximately 1% that of the wind response scale, it is important to consider how far upwave the nearest trough is when studying any particular shelf circulation.

3.4 Troughs Enhance Upwelling of Slope Waters to the Shelf

An upwave-oriented wind forcing will drive upwelling and produce alongshore currents that move upwave. This upwave-oriented configuration is opposite to the results examined thus far, where wind forcing over the shelf is pointed downwave and, in turn, causes shelf flows to move downwave. Because the model is linear, the model solutions are identical in all respects except for the reversal of the currents.

The right panel of Figure 2 can be examined by imagining the forcing is directed upwave, instead of downwave in this figure, to understand how upwave-oriented slope flows would be impacted by a trough. The presence of the trough causes these slope flows to cross isobaths, moving onshore to shallower isobaths upwave of the trough. Note that only the streamlines on the slope at depths shallower than the trough depth are moved onto the shelf. This can be seen in the figure, where streamlines on the slope offshore of that depth are only slightly altered by the trough. This baseline-parameter trough absorbs slope transport to the shelf, resulting in a 53% increase in shelf transport upwave of the trough, as compared to the transport on the shelf downwave of the trough.

Recall that forcing is communicated via propagation of coastal trapped waves, which move with shallows on the right in the northern hemisphere (southwards for this western-boundary shelf). This remains true for both upwelling-favorable and downwelling-favorable cases. Whether winds are oriented upwave or downwave, only the waters downwave of these winds will adjust to the forcing because of the asymmetric communication of the forcing. Therefore, the results that demonstrated how far downwave of a trough its impact must be considered are equally valid for forcing/flows of either downwave or upwave orientation.

4 Discussion

4.1 Trough-Enhanced Downwelling and Upwelling of Shelf Flows, and Implications

Shelf currents that move downwave (in the direction of coastal trapped waves) are largely ejected offshore to the slope by troughs (Figure 2). These flows, which were forced by downwave-oriented winds over the shelf, encounter the trough and attempt to navigate around it because linear flows follow isobaths on an f-plane. Upon navigating around this trough bathymetry, relative vorticity is generated and introduced to the system. Bottom friction works to dissipate this relative vorticity, and in turn, causes the migration of shelf flows off their isobaths to deeper waters. This migration occurs through a downwelling Ekman bottom transport. The net effect is that shelf transport is ejected offshore to the slope.

The trough geometry parameters that most impact the shelf to slope transport are those that control the narrowing of isobaths. Therefore, the trough parameters that most control ejection of shelf flows are the alongshore trough width, and the distance between the trough head and the coast. A trough that intersects most of the shelf, and extends a large alongshore distance, will make a more significant impact on coastal circulation than one which is narrow in the alongshore, and resides far offshore. A trough which exhibits this significant geometry, and indeed drastically alters coastal circulation, is the Laurentian Channel. The southward-moving flows from the Labrador Sea are swiftly ejected offshore to slope, resulting in a sharp boundary of different shelf circulation types at this bathymetric boundary (Dever et al., 2016). The opposite case to this (alongshore narrow and far offshore) are extreme cases of river-carved canyons, which do not greatly affect flow on the shelf. It is only when canyons begin to cut across much of the shelf that their impact on shelf circulation becomes consequential; the Hudson Canyon is an example of such an exceptional river-carved canyon (Zhang & Lentz, 2017).

There are multiple secondary effects on ocean dynamics due to this trough ejection of shelf transport to the slope (Fratantoni & Pickart, 2007; Greatbatch et al., 1995;

Greenberg & Petrie, 1988; Han et al., 2008). One example is that the exchange of shelf waters to the slope by a trough will impact the chemical compositions of both sets of waters. Shelf waters are home to significant biological communities and physical exchange properties. Therefore, troughs are expected to move alongshelf waters to the deeper slope waters (at least in the weakly stratified case), bringing with it its physical, chemical, and biological constituents. For example, the exchange of carbon through this downwelling will contribute to the global carbon cycle (Holt et al., 2009). Any other secondary phenomenon that would be impacted by the downwelling of shelf waters should consider the role of troughs, especially at higher latitudes where troughs are highly concentrated.

Because this model is linear, the upwelling case with upwave flowing currents is the same as the downwelling case with downwelling currents, but with the flow reversed. Thus, in the upwelling case, flow is not ejected from the shelf, but is absorbed from the slope onto the shelf. The baseline-parameter trough will cause an increase of 53% of shelf flow upwave by enhancing upwelling from the slope. Note that only flows along the slope that are at or shallower than the trough's deepest isobath will be directly impacted.

Trough-enhanced upwelling of flows onto the shelf will have substantial impacts on ocean dynamics. For example, warm slope waters that upwell via a trough into the Amundsen Sea account for most of the heating, and subsequent basal melting, of the entire West Antarctic Ice Shelf region (Wåhlin et al., 2013; Walker et al., 2007). Additionally, the troughs along the Greenland Shelf significantly contribute to both nutrient cycling within those local coastal waters (Cape et al., 2019), and ice melt (Rysgaard et al., 2020). Both the exchange of heat and nutrients between the shelf and deeper waters by a trough are lowest order ocean dynamics: dynamics which impact glacial-mass balances, biological populations within coastal waters, etc. The combination of upwelling of slope waters to the shelf, and steering of such flows between the trough head and the coast through the trough narrowing mechanism, enhances the presence of slope waters onshore of the trough. Because fjord locations may likely contain a glacial tongue, this mechanism could contribute to glacial melt. Additionally, troughs upwelling deeper waters onto the shelf could largely contribute to biological processes, because of deeper waters being rich in nutrients.

Although the literature attributes these observations of trough-induced upwelling to buoyancy forcing, this study demonstrates that troughs can cause upwelling even in the unstratified limit. Therefore, observations of trough-driven circulation patterns should not be reduced to buoyancy forcing alone. Barotropic dynamics must be accounted for.

In light of this trough-induced absorption, two conclusions can now be made in total about a trough's impact on coastal circulation: 1) a trough will cause downwave-moving shelf flows to eject offshore to the slope through downwelling, and 2) a trough will cause upwave-moving slope flows to absorb onshore to the shelf through upwelling.

4.2 How Far Alongshore Does the Trough Impact Remain Significant?

The trough ejection and absorption impacts will be lowest order effects on coastal circulation within the alongshore trough-adjustment-scale of a trough. This was demonstrated by this model's baseline-parameter trough, which caused an O(50%) change in shelf transport. The alongshore scaling of these trough dynamics, as compared to that of wind forcing, demonstrates that the trough impact will remain relevant for hundreds of kilometers downwave of a trough. Whereas the trough ejection/absorption impact acts on an alongshore scale of O(10s km), the alongshore scale of wind response is known to be: $L_{fric} = -\frac{Hf}{2r}L^x$ (Chapman, 1986). The appropriate depth scale for H to understand shelf adjustment is the shelfbreak depth. The appropriate offshore length scale for L^x is the shelf width. Therefore, it can be concluded that a shelf with a shallower shelfbreak depth and a narrower offshore extent will have a shorter alongshore scale of adjustment to wind forcing. For shelves with this structure, the trough impact will remain relevant for a lesser alongshore distance downwave of the trough, because the shelf will more quickly adjust to wind forcing. Conversely, a wide shelf with a deep shelfbreak depth will be subject to the trough impact for a longer distance downwave of trough.

The other two parameters that drive this alongshore response scale are f, the Coriolis frequency, and r, the bottom linear drag coefficient. The trough impact will remain significant for longer alongshore distances at high latitudes, given that f increases with higher latitude. Finally, stronger linear bottom friction (greater linear drag coefficient r) will decrease the alongshore distance that the trough impact remains significant because it is inversely proportional; the linear drag coefficient r is typically $2{-}5{*}10^{-4}\frac{m}{s}$ (Williams & Carmack, 2008).

The results of a back-of-the-envelope calculation of the alongshore wind response scale (L_{fric}) for three specific shelves are considered: that of the Scotian Shelf, the shelf along southwestern Greenland, and the Antarctic Shelf directly south of Africa. Appropriate Coriolis frequency values were chosen for each, as well as a linear drag coefficient value of $5*10^{-4}\frac{m}{s}$, and a shelfbreak depth of 200 m. The Scotian Shelf, with a width of approximately 150 km, has an alongshore response scale of O(3000 km), the southern Greenland Shelf, with a width of approximately 40 km, has an alongshore response scale of O(1000 km), and the Antarctic Shelf (near 15°E), with a width of approximately 10 km, has an alongshore response scale of O(250 km). These three cases show that the alongshore extent of the trough impact can vary wildly depending on a shelf's bathymetry.

In addition to considering this alongshore scale, which depends on a shelf's parameters, the frequency of troughs should be considered. Every time flows encounter a trough, they are subject to the trough impact. The most recent trough encountered by flows is the trough that sets the alongshore scale of relevance. Therefore, upon considering how far the extent of a trough-driven impact on shelf flows is, one must consider the most nearby trough in the upwave direction. Shelves with more troughs will be subject to these trough impacts more significantly. But, once troughs are more closely spaced than the alongshore scale of their impact, additional troughs will have little additional impact. Streamlines are more tightly constrained to isobaths at high latitudes because of the stronger Coriolis parameter, and troughs exist in higher abundance on glaciated/previously-glaciated shelves at these high latitudes (Harris & Whiteway, 2011). Therefore, troughs will be an even greater inhibition on wind-driven circulation on high-latitude shelves.

4.3 Where Does the Model Fail?

Results from this model demonstrate that troughs enhance the ejection of downwave-moving shelf transport to the slope (and enhance the absorption of upwave-moving slope waters to the shelf). Extrapolation of these results to shelf systems can only be done if the system resides within this model's physical regime. The following reiterates the physical limits of this model and describes how to apply these results within these limits.

This model is of coastal flows in the steady-state limit, which depends on the underlying forcing being at a steady-state. Rather than describing the dynamics of adjustment, as flows respond to some changing forcing, these results describe how that adjusted state behaves. If a wind forcing changes against what was previously steady, such as a winter storm forcing differently than the seasonal average, then the flows will start to adjust to this new forcing. If this forcing remains stable for a long enough time for the flows to adjust into a steady-state, then these results will once again become relevant. The time scale to determine if flows have reached a steady-state after adjusting to a forcing is the frictional spindown time: $\frac{H}{r}$, where H is the depth of a water column, and r is the linear drag coefficient (Williams & Carmack, 2008). In order to understand the timescale for an entire shelf to adjust, an appropriate choice of H is the shelfbreak depth. The choice of linear drag coefficient, r, must be chosen as an empirically representative value of a shelf system of interest. Recall that this linear drag coefficient is typically in the range of $2 - 5 * 10^{-4} \frac{m}{s}$ (Williams & Carmack, 2008). For example, a shelf with a shelfbreak depth (H) of 100 m and a linear drag coefficient (r) of $5 * 10^{-4} \frac{m}{s}$, the frictional spindown time is $2{*}10^5 s$ or approximately 2.3 days. Therefore, flows on a shelf of this nature will adjust to a steady-state in approximately two days, for the values given here.

The results of this model are in the barotropic limit. As the internal radius of deformation becomes small relative to the shelf, or the equivalent limit of the slope Burger Number, dynamics of flows approach the barotropic limit. For example, the structure of low mode CTW on the shelf approaches the barotropic limit (Brink, 1991). Likewise, the effects of bottom boundary layer shutdown become small (Trowbridge & Lentz, 1991). Most relevant to this work, the bathymetric effects on upwelling become barotropic in these limits (Janowitz & Pietrafesa, 1982). Thus, in the limit that the internal radius of deformation is small compared to the width of the shelf, and, more restrictively, the horizontal length scales of the trough are large compared to the radius of deformations, these results should apply, at least qualitatively.

The final core limit of this model is that these shelf flows are linear. This occurs when the Rossby number is small: $\frac{u}{fL} << 1$. The Rossby number at the upwave boundary of this model, based on the 10 $\frac{cm}{s}$ inflow over a 150 km wide shelf, is approximately 0.006, i.e., strongly linear. The Rossby number begins to increase in this system where the shelf flows are constricted into the narrowed shelf, between the trough head and coast. Flows are accelerated to a magnitude of approximately 30 $\frac{cm}{s}$ across this 25 km shelf (in the case of baseline input parameters), giving a Rossby number of 0.12, i.e., approaching a nonlinear scale. In the variation-run results, where the offshore distance to the trough head was varied, the Rossby number greatly increases as the trough extent goes to the coast. A 1 km wide narrowed shelf, where the trough essentially merges with the coast, gives a Rossby number of 3. For this system, the details of the flow structure are not properly accounted by this linear model. Therefore, currents of significant magnitude over significantly narrow shelves are better described by nonlinear studies. An examination of nonlinear circulation in the Arctic demonstrated how cross-shore exchange between the shelf and the slope occurs in this limit (Williams et al., 2001).

5 Conclusions

Much of the current understanding of coastal circulation dynamics comes from studying baroclinic dynamics and/or wind forcing (Csanady, 1978; Pringle, 2018), as well as dynamics associated with river-carved canyons (Allen & Hickey, 2010). The contributions of glacial troughs to coastal circulation dynamics have been largely overlooked, despite observations indicating their significance (Buhl-Mortensen et al., 2012; Cape et al., 2019; Wåhlin et al., 2013; Walker et al., 2007). Model results explored in this study affirm that troughs significantly impact coastal circulation dynamics. Although troughs may drive the exchange between the slope and shelf through baroclinic processes, as demonstrated by these cited studies, this model demonstrates that the exchange can occur within the barotropic limit.

Troughs enhance the offshore ejection of barotropic shelf flows to the slope during downwelling-favorable downwave flows (and onshore absorption during upwelling-favorable upwave flows) by generating relative vorticity, which bottom friction dissipates and causes cross-shore migration of currents. Relative vorticity is generated because linear flows navigate around the trough, attempting to maintain their isobaths, which occurs most strongly where isobaths narrow. Therefore, there are two trough dimensions that will most dictate the strength of its impact on coastal circulation: alongshore trough width, and offshore expanse of the trough across the shelf.

This model characterized how far downwave these trough dynamics remain significant, by contrasting its alongshore response scale to that of wind forcing . This trough impact distance can range from O(100 km) on narrow shelves like parts of the Antarctic to O(1500 km) on wide shelves like the Scotian. This alongshore distance should be measured in relation to the closest trough upwave.

The cross-shelfbreak exchange of flows driven by a trough can dominate cross-shelfbreak exchange local to, and downwave of, such trough. This enhanced exchange will greatly modify processes that depend on the exchange of flows between the shelf and slope. For example, troughs downwelling shelf flows to the slope could be an important mechanism in the carbon pump, as well as driving biological growth on the shelf in the case of troughs upwelling nutrient-rich waters from depths below (Cape et al., 2019; Holt et al., 2009). Troughs enhancing the upwelling of warmer slope currents to the cooler shelf, and the subsequent concentration of these waters onshore into a fjord region, could enhance glacial melting (Rysgaard et al., 2020; Wåhlin et al., 2013; Walker et al., 2007). Model results explored here show that troughs upwell flows along isobaths shallower than the deepest depths of the trough. The upwelling, and subsequent exchange of slope flows from depths below the trough, must first be brought up by some other mechanism. Finally, as troughs cause currents to migrate offshore towards the slope, this will be one cause of the shelfbreak jet (Fratantoni & Pickart, 2007; Greatbatch et al., 1995; Greenberg & Petrie, 1988; Han et al., 2008).

This study shows that troughs can significantly impact coastal circulation. An increased understanding of how significantly the trough impact is will come as these results are applied to observations, and this study is expanded beyond these physical limits, i.e., the barotropic, linear, and steady-state dynamics explored here.

Acknowledgments

This material is based upon work supported by the National Science Foundation under OCE-1459609. No new data were used in producing this manuscript. The code for the numerical model is provided in the supplementary information.

References

Allen, S. E., & Hickey, B. M. (2010). Dynamics of advection-driven upwelling over a shelf break submarine canyon. *Journal of Geophysical Research: Oceans*, *115*(C8). doi: 10.1029/2009JC005731

Battisti, D. S., & Hickey, B. M. (1984). Application of Remote Wind-Forced Coastal Trapped Wave Theory to the Oregon and Washington Coasts. *Journal of Physical Oceanography*, *14*(5), 887–903. doi: 10.1175/1520-0485(1984)014⟨0887:AORWFC⟩2.0.CO;2

Brink, K. H. (1991). Coastal-Trapped Waves and Wind-Driven Currents Over the Continental Shelf. *Annual Review of Fluid Mechanics*, *23*(1), 389–412. (_eprint: https://doi.org/10.1146/annurev.fl.23.010191.002133) doi: 10.1146/annurev.fl.23.010191.002133

Brink, K. H., & Allen, J. S. (1978). On the Effect of Bottom Friction on Barotropic Motion Over the Continental Shelf. *Journal of Physical Oceanography*, *8*(5), 919–922. doi: 10.1175/1520-0485(1978)008⟨0919:OTEOBF⟩2.0.CO;2

Buhl-Mortensen, L., Bøe, R., Dolan, M. F. J., Buhl-Mortensen, P., Thorsnes, T., Elvenes, S., & Hodnesdal, H. (2012). 51 - Banks, Troughs, and Canyons on the Continental Margin off Lofoten, Vesterålen, and Troms, Norway. In P. T. Harris & E. K. Baker (Eds.), *Seafloor Geomorphology as Benthic Habitat* (pp. 703–715). London: Elsevier. doi: 10.1016/B978-0-12-385140-6.00051-7

Cape, M. R., Straneo, F., Beaird, N., Bundy, R. M., & Charette, M. A. (2019). Nutrient release to oceans from buoyancy-driven upwelling at Greenland tidewater glaciers. *Nature Geoscience*, *12*(1), 34–39. doi: 10.1038/s41561-018-0268-4

Chapman, D. C. (1985). Numerical Treatment of Cross-Shelf Open Boundaries in a Barotropic Coastal Ocean Model. *Journal of Physical Oceanography*, *15*(8), 1060–1075. doi: 10.1175/1520-0485(1985)015⟨1060:NTOCSO⟩2.0.CO;2

Chapman, D. C. (1986). A Simple Model of the Formation and Maintenance of the Shelf/Slope Front in the Middle Atlantic Bight. *Journal of Physical Oceanog-*

raphy, *16*(7), 1273–1279. doi: 10.1175/1520-0485(1986)016⟨1273:ASMOTF⟩2.0.CO;2

Chapman, D. C., & Gawarkiewicz, G. (2012). Offshore transport of dense shelf water in the presence of a submarine canyon. *Journal of Geophysical Research: Oceans*, *100*(C7), 13373–13387. doi: 10.1029/95JC00890

Csanady, G. T. (1978). The Arrested Topographic Wave. *Journal of Physical Oceanography*, *8*(1), 47–62. doi: 10.1175/1520-0485(1978)008⟨0047:TATW⟩2.0.CO;2

Dever, M., Hebert, D., Greenan, B. J. W., Sheng, J., & Smith, P. C. (2016). Hydrography and Coastal Circulation along the Halifax Line and the Connections with the Gulf of St. Lawrence. *Atmosphere-Ocean*, *54*(3), 199–217. doi: 10.1080/07055900.2016.1189397

Fratantoni, P., & Pickart, R. (2007). The Western North Atlantic Shelfbreak Current System in Summer. *Journal of Physical Oceanography*(10), 2509. doi: 10.1175/JPO3123.1

Gawarkiewicz, G., & Chapman, D. C. (1991). Formation and Maintenance of Shelfbreak Fronts in an Unstratified Flow. *Journal of Physical Oceanography*, *21*(8), 1225–1239. doi: 10.1175/1520-0485(1991)021⟨1225:FAMOSF⟩2.0.CO;2

Gordon, R. L. (1982). Coastal ocean current response to storm winds. *Journal of Geophysical Research: Oceans*, *87*(C3), 1939–1951. doi: 10.1029/JC087iC03p01939

Greatbatch, R. J., Pal, B. K., & Ren, Y. (1995). Experiments using a long-time-scale shelf circulation model of relevance to the Labrador Current. *Continental Shelf Research*, *15*(1), 41–57. doi: 10.1016/0278-4343(94)P1812-P

Greenberg, D. A., & Petrie, B. D. (1988). The mean barotropic circulation on the Newfoundland shelf and slope. *Journal of Geophysical Research: Oceans*, *93*(C12), 15541–15550. doi: 10.1029/JC093iC12p15541

Han, G., Lu, Z., Wang, Z., Helbig, J., Chen, N., & Young, B. d. (2008). Seasonal variability of the Labrador Current and shelf circulation off Newfoundland. *Journal of Geophysical Research: Oceans*, *113*(C10). doi: 10.1029/2007JC004376

Harris, P. T., & Whiteway, T. (2011). Global distribution of large submarine canyons: Geomorphic differences between active and passive continental margins. *Marine Geology*, *285*(1), 69–86. doi: 10.1016/j.margeo.2011.05.008

Holt, J., Wakelin, S., & Huthnance, J. (2009). Down-welling circulation of the northwest European continental shelf: A driving mechanism for the continental shelf carbon pump. *Geophysical Research Letters*, *36*(14). doi: 10.1029/2009GL038997

Huthnance, J. M. (1975). On trapped waves over a continental shelf. *Journal of Fluid Mechanics*, *69*(4), 689–704. (Publisher: Cambridge University Press) doi: 10.1017/S0022112075001632

Janowitz, G. S., & Pietrafesa, L. J. (1982). The effects of alongshore variation in bottom topography on a boundary current—(topographically induced upwelling). *Continental Shelf Research*, *1*(2), 123–141. doi: 10.1016/0278-4343(82)90001-2

Lentz, S., Guza, R. T., Elgar, S., Feddersen, F., & Herbers, T. H. C. (1999). Momentum balances on the North Carolina inner shelf. *Journal of Geophysical Research: Oceans*, *104*(C8), 18205–18226. doi: 10.1029/1999JC900101

Price, J. F. (2003). Dimensional analysis of models and data sets. *American Journal of Physics*, *71*(5), 437–447. doi: 10.1119/1.1533057

Pringle, J. M. (2002). Enhancement of Wind-Driven Upwelling and Downwelling by Alongshore Bathymetric Variability. *Journal of Physical Oceanography*, *32*(11), 3101–3112. doi: 10.1175/1520-0485(2002)032⟨3101:EOWDUA⟩2.0.CO;2

Pringle, J. M. (2018). Remote Forcing of Shelf Flows by Density Gradients and the Origin of the Annual Mean Flow on the Mid-Atlantic Bight. *Journal of Geophysical Research: Oceans*, *123*(7), 4464–4482. doi: 10.1029/2017JC013721

Rysgaard, S., Boone, W., Carlson, D., Sejr, M. K., Bendtsen, J., Juul-Pedersen, T., … Mortensen, J. (2020). An Updated View on Water Masses on the pan-West Greenland Continental Shelf and Their Link to Proglacial Fjords. *Journal of Geophysical Research: Oceans*, *125*(2), e2019JC015564. doi: 10.1029/2019JC015564

Sandstrom, H. (1980). On the wind-induced sea level changes on the Scotian shelf. *Journal of Geophysical Research: Oceans*, *85*(C1), 461–468. doi: 10.1029/JC085iC01p00461

Stommel, H. (1948). The westward intensification of wind-driven ocean currents. *Eos, Transactions American Geophysical Union*, *29*(2), 202–206. doi: 10.1029/

TR029i002p00202

Straneo, F., Curry, R. G., Sutherland, D. A., Hamilton, G. S., Cenedese, C., Våge, K., & Stearns, L. A. (2011). Impact of fjord dynamics and glacial runoff on the circulation near Helheim Glacier. *Nature Geoscience*, *4*(5), 322–327. doi: 10.1038/ngeo1109

Trowbridge, J. H., & Lentz, S. J. (1991). Asymmetric Behavior of an Oceanic Boundary Layer above a Sloping Bottom. *Journal of Physical Oceanography*, *21*(8), 1171–1185. (Publisher: American Meteorological Society Section: Journal of Physical Oceanography) doi: 10.1175/1520-0485(1991)021⟨1171:ABOAOB⟩2.0.CO;2

Walker, D. P., Brandon, M. A., Jenkins, A., Allen, J. T., Dowdeswell, J. A., & Evans, J. (2007). Oceanic heat transport onto the Amundsen Sea shelf through a submarine glacial trough. *Geophysical Research Letters*, *34*(2). doi: 10.1029/2006GL028154

Williams, W. J., & Carmack, E. C. (2008). Combined effect of wind-forcing and isobath divergence on upwelling at Cape Bathurst, Beaufort Sea. *Journal of Marine Research*, *66*(5), 645–663. doi: 10.1357/002224008787536808

Williams, W. J., Gawarkiewicz, G. G., & Beardsley, R. C. (2001). The adjustment of a shelfbreak jet to cross-shelf topography. *Deep Sea Research Part II: Topical Studies in Oceanography*, *48*(1), 373–393. doi: 10.1016/S0967-0645(00)00085-0

Wright, D. G., & Thompson, K. R. (1983). Time-Averaged Forms of the Nonlinear Stress Law. *Journal of Physical Oceanography*, *13*(2), 341–345. doi: 10.1175/1520-0485(1983)013⟨0341:TAFOTN⟩2.0.CO;2

Wåhlin, A. K., Kalén, O., Arneborg, L., Björk, G., Carvajal, G. K., Ha, H. K., ... Stranne, C. (2013). Variability of Warm Deep Water Inflow in a Submarine Trough on the Amundsen Sea Shelf. *Journal of Physical Oceanography*, *43*(10), 2054–2070. doi: 10.1175/JPO-D-12-0157.1

Zhang, W. G., & Lentz, S. J. (2017). Wind-Driven Circulation in a Shelf Valley. Part I: Mechanism of the Asymmetrical Response to Along-Shelf Winds in Opposite Directions. *Journal of Physical Oceanography*, *47*(12), 2927–2947. doi: 10.1175/JPO-D-17-0083.1

704 # Tables

Table 1. Model input parameters′ baseline values, as well as minima, maxima, and increments used in variation-runs.

Parameter	Baseline value	Minimum[a]	Maximum[a]	Step size[a]
$r[\frac{m}{s}]$	0.005	0.002	0.01	0.001
$f[\frac{1}{s}]$	0.001	0.0001	0.0015	0.0001
$H_{trough}[m]$	250	0	600	50
$L_{head}[km]$	20	0	150	10
$L_{shelf}[km]$	150	100	180	5
$W_{trough}[km]$	50	0	150	10

[a]Applies to the variation-runs.

705 # Figures

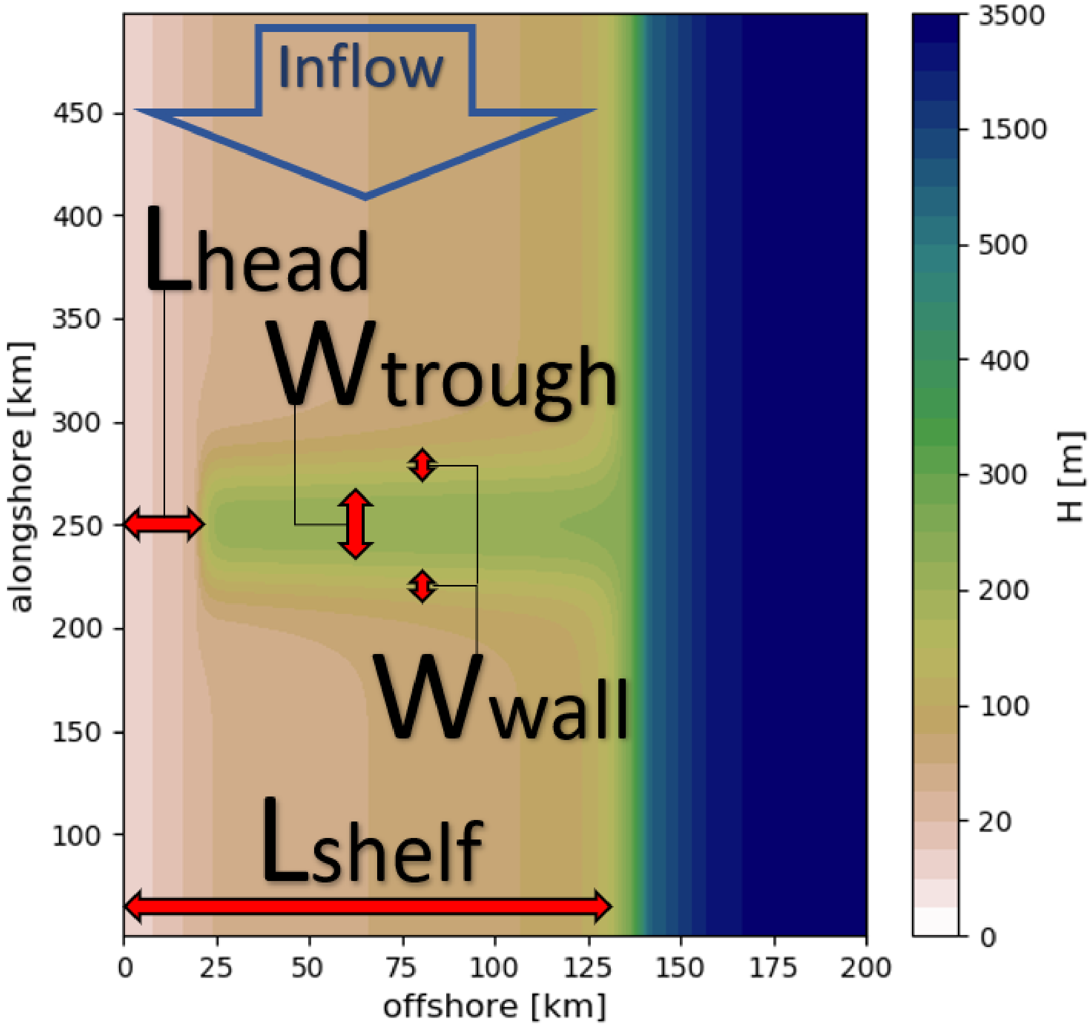

Figure 1. Model bathymetry includes a trough on the shelf. The key geometric parameters that define the trough and shelf system are labeled with red cartoon-arrows. The upwave forcing of wind-generated shelf flows is labeled with a blue cartoon-arrow.

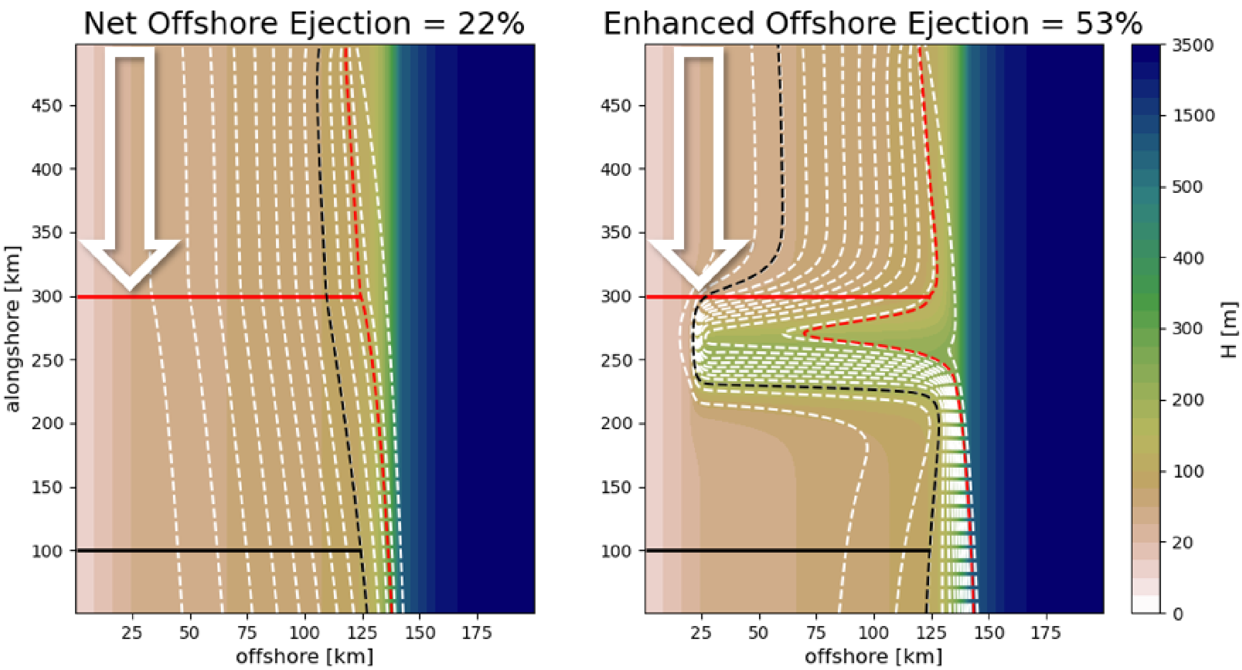

Figure 2. Resulting streamlines of two model runs are plotted as white dashed lines. Streamlines plotted on this and other figures in this paper are uniformly spaced in Ψ (streamline). On the left is of a run without a trough, and on the right is one with a baseline-parameter trough. White cartoon arrows are included to represent the shelf wind forcing, which is confined to only the shelf upwave of the trough location. Loss of shelf transport to the slope is quantified by calculating the difference in flow from the upwave (red) transect to the downwave (black) transect.

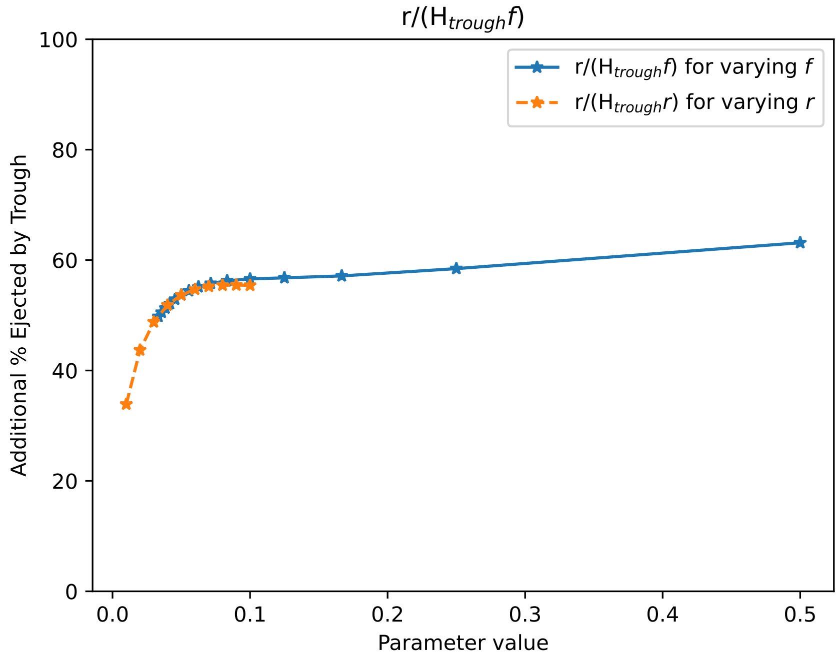

Figure 3. The impact of changes in the Coriolis parameter, f, and the bottom friction, r, on offshore ejection. As $r/(H_{trough}f)$ increases, the offshore ejection increases. An increase in bottom friction increases the rate at which relative vorticity is dissipated by bottom friction to cause cross-shelf transport, while an increase in the Coriolis parameter increases the amount of vorticity that must be dissipated to allow this transport.

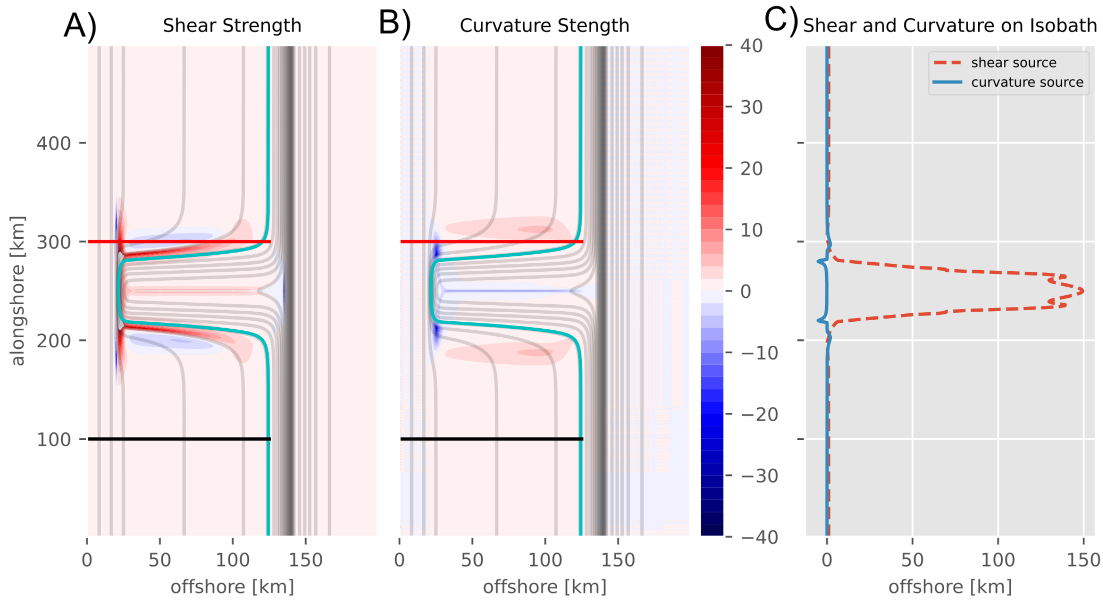

Figure 4. The relative strength of the cross-isobath transport for the baseline trough case, as caused by A), enhanced shear caused by narrowing isobaths as estimated by equation (16), B), curving isobaths, as estimated by equation (17), and C), these two terms along the shelfbreak isobath (marked in cyan in panels A and B). To convert these scaled transports to the actual transport, they must be multiplied by the Ekman transport given by the upwave wind forcing.

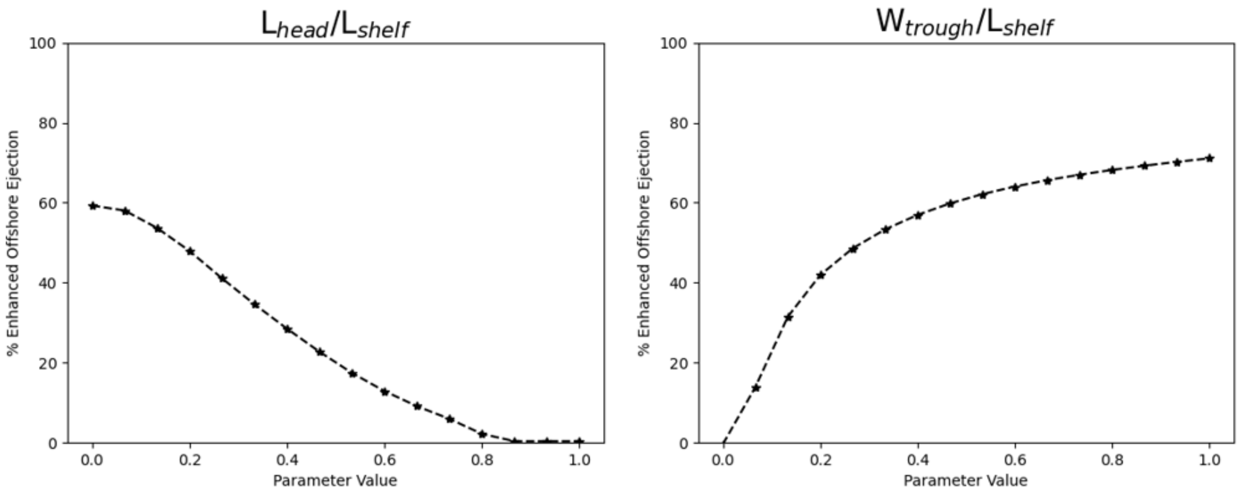

Figure 5. Two different parameter variation results are plotted here to show the impact of the narrowing source on offshore ejection, i.e., change in ejection as a function of parameter value change. On the left is the parameter $\frac{L_{head}}{L_{shelf}}$, which controls the magnitude of velocity shear, reaching a maximum as the shelf width narrows to zero, and reaching a minimum as the trough disappears to the slope. On the right is the parameter $\frac{W_{trough}}{L_{shelf}}$, which controls the accumulation of the shear impact. Ejection change is directly proportional to this parameter (trough width), because a longer alongshore distance allows for a higher accumulation of the shear impact. An O(1) change in both parameters alters offshore ejection by approximately 60%.

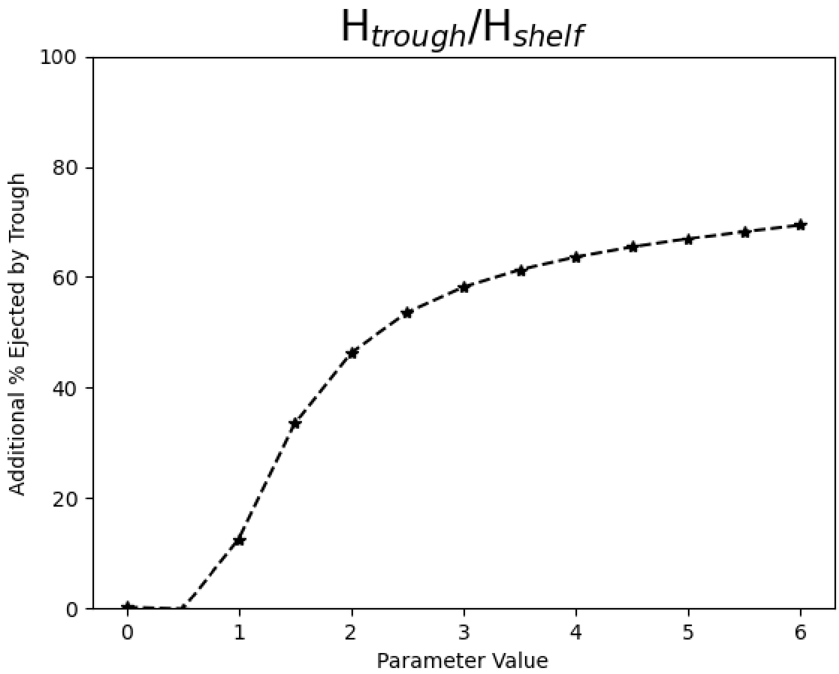

Figure 6. The impact of the trough depth (relative to the shelf depth) on offshore ejection. As the parameter $\frac{H_{trough}}{H_{shelf}}$ increases, the offshore ejection by the trough increases. This is because the more significant the change in depth that alongshore flows encounter at the trough, the more tightly constrained they will be on shallower shelf isobaths. This tighter constraining to the shelf will cause an increase in the narrowing mechanism, as more of the flow is constrained around the trough, and thus, more transfer of transport from the shelf to the slope.

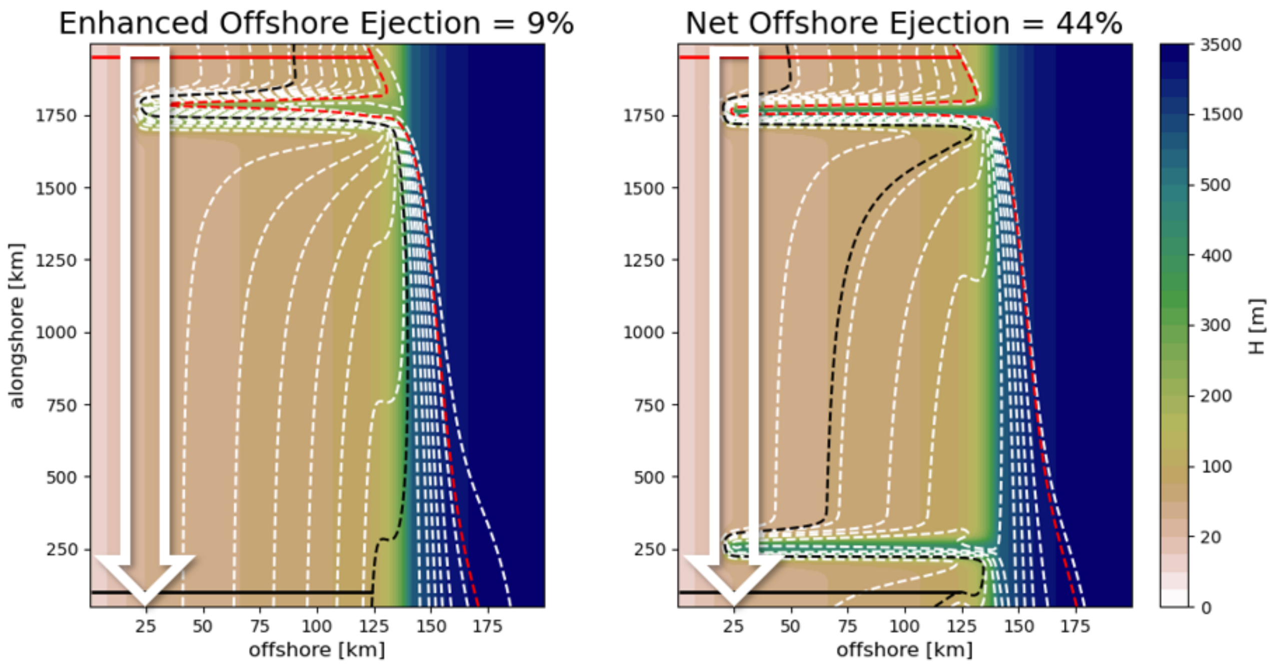

Figure 7. Resulting streamlines of two model runs are plotted above: one with a single trough (left) and one with two troughs (right). White cartoon arrows are included to represent the wind forcing, which extends over the entire shelf domain. Loss of shelf transport to the slope is quantified by calculating the difference in flow from the upwave (red) transect to the downwave (black) transect.